J Mol Model (2013) 19:4689–4700
DOI 10.1007/s00894-012-1505-1

ORIGINAL PAPER

# Regulation of the transient receptor potential channel TRPA1 by its N-terminal ankyrin repeat domain

**Vasilina Zayats · Abdul Samad · Babak Minofar · Katherine E. Roelofs · Thomas Stockner · Rudiger Ettrich**

Received: 23 December 2011 / Accepted: 13 June 2012 / Published online: 3 July 2012


**Abstract** The transient receptor potential channel A1 (TRPA1) is unique among ion channels of higher vertebrates in that it harbors a large ankyrin repeat domain. The TRPA1 channel is expressed in the inner ear and in nociceptive neurons. It is involved in hearing as well as in the perception of pungent and irritant chemicals. The ankyrin repeat domain has special mechanical properties, which allows it to function as a soft spring that can be extended over a large range while maintaining structural integrity. A calcium-binding site has been experimentally identified within the ankyrin repeats. We built a model of the N-terminal 17 ankyrin repeat structure, including the calcium-binding EF-hand. In our simulations we find the calcium-bound state to be rigid as compared to the calcium-free state. While the end-to-end distance can change by almost 50% in the apo form, these fluctuations are strongly reduced by calcium binding. This increase in stiffness that constraints the end-to-end distance in the holo form is predicted to affect the force acting on the gate of the TRPA1 channel, thereby changing its open probability. Simulations of the transmembrane domain of TRPA1 show that residue N855, which has been associated with familial episodic pain syndrome, forms a strong link between the S4-S5 connecting helix and S1, thereby creating a direct force link between the N-terminus and the gate. The N855S mutation weakens this interaction, thereby reducing the communication between the N-terminus and the transmembrane part of TRPA1.

**Keywords** Ankyrin repeat · EF-hand · Familial episodic pain syndrom · TRPA1

**Electronic supplementary material** The online version of this article (doi:10.1007/s00894-012-1505-1) contains supplementary material, which is available to authorized users.

V. Zayats · A. Samad · B. Minofar · R. Ettrich
Institute of Nanobiology and Structural Biology of GCRC,
Academy of Sciences of the Czech Republic,
Zamek 136,
37333 Nove Hrady, Czech Republic

V. Zayats · B. Minofar · R. Ettrich
Faculty of Sciences, University of South Bohemia in Ceske Budejovice,
Zamek 136,
37333 Nove Hrady, Czech Republic

K. E. Roelofs
Princeton University,
Princeton, NJ, USA

T. Stockner (✉)
Center for Physiology and Pharmacology,
Institute of Pharmacology, Medical University Vienna,
Waehringerstrasse 13a,
1090 Vienna, Austria
e-mail: thomas.stockner@meduniwien.ac.at

## Introduction

Transient receptor potential (TRP) channels are a large superfamily of nonselective cation channels that play an important role in many sensory functions. The TRP cation channel, subfamily A, member 1, (TRPA1) is a protein of 1119 amino acids (in human) with the molecular weight of 127.4 kDa [1]. It is expressed in hair cell epithelia of the inner ear [2] and the nociceptive neurons [1]. A distinguishing feature of TRPA1 is its long N-terminus with 14-18 predicted ankyrin repeats [1, 3–6]. The only other TRP protein with a comparable number of repeats is the mechanosensory channel TRPN1, which is not present in genomes of higher vertebrates. Ankyrin repeats [7, 8] represent a short motif of 33 amino acids which have a conserved sequence and three-dimensional architecture with an antiparallel helix-turn-helix motif followed by a hairpin loop. Ankyrin repeats have long been implicated in protein-protein interactions, elasticity, and forming molecular springs [9].

TRPA1 can be activated by many different stimuli including exogenous pungent compounds and irritants, bradykinin and other endogenous proalgesic agents, cold, and by mechanical force [1, 6, 10–13]. Animal models indicate that TRPA1 is the only sensor that is activated by respiratory irritants at acute exposure [13–16]. Calcium ions have been reported to directly activate TRPA1 through binding to an EF-hand [17, 18]. TRPA1 channels can be regulated by phosphatidylinositol bisphosphate (PIP2) [19, 20], which is present in the inner leaflet of cell membranes, where it constitutes ~1% of lipids.

The remarkable elastic properties of ankyrin repeats have been studied experimentally by AFM microscopy [9, 21] and by steered molecular dynamics simulations [4, 22], showing that the protein can extend over a range of 5-10 nm while keeping structural integrity.

In this study, we present a model of the N-terminal domain of TRPA1 containing 17 ankyrin repeats and the EF-hand calcium-binding domain, as well as the transmembrane domains. We find that binding of calcium to the EF-hand translates into a change in the overall flexibility and into a preference for long end-to-end distances, which we find to range between 6 and 11 nm in the apo form, and between 8.5 and 11.5 nm in the calcium-bound form. We propose that the multifunctional sensory properties of the N-terminus of TRPA1 do all translate into a change in the force acting onto the gate.

## Materials and methods

### Model generation

#### *N-terminal*

We selected the human ankyrinR [23] (PDB ID: 1N11) as a template for modeling of hTRPA1, as it contains 12 ankyrin repeats and shows ~25% identity to the ankyrin repeats of the TRPA1 channel. We doubled the 1N11 structure to obtain a template for the full length ankyrin repeat of TRPA1. Ankyrin repeats are conserved motifs, which possess the canonical pattern [G-(X)-TPLH-(X)-A-(X3)-G-(X7)-LL-(X2)-GA-(X5)]. Ankyrin repeat identification, secondary structure prediction and alignment were done using ProteinPredict [24], HHpred [25], I-TASSER [26], Phyre [27], and ClustalW [28]. The final alignment used for modeling is shown in supplemental Fig. 1 of online resource 1. Conservation of the ankyrin repeat pattern revealed that TRPA1 contains 17 ankyrin repeats. Model building was done using MODELLER [29].

A calcium-binding EF-hand was identified and verified by site-directed mutagenesis [17]. The coordinates of a human calprotectin EF-hand (PDB ID: 1XK4) [30] were placed accordingly. Models of the TRPA1 ankyrin repeats were created using the automodel procedure of MODELLER [29]. The quality of the calculated models was assessed using Procheck [31], Prosa [32] and the MODELLER objective function.

#### *TM domain*

The crystal structure of the Kv1.2 potassium channel [33] (PDB ID: 3LUT) was used as a template for building a model of the transmembrane domain (TM) of TRPA1. TM helices were identified using TMHMM [34], PredictProtein [24], and TMpred [35]. The sequence alignment was carried out by ClustalW [28], T-Coffee [36], and Muscle [37] and manually adjusted. TM helix predictions as well as the final alignment are shown in the supplement Figs. 2 and 3 of online resource 1, respectively. Models were built using YASARA [38]. Model quality was assessed using the Z-score provided by YASARA.

### Simulations

The selected model of N-terminal ankyrin repeat domain was inserted into a water box for all atom molecular dynamics simulation (MD). Two simulations were carried out - for calcium-bound, and calcium-free state. The OPLS all-atom force field was used. Water was represented by the SPC [39] water model. All simulations were performed using the Gromacs 4 MD package [40, 41]. The integration time step was set to 2 fs. Periodic boundary conditions were applied in all dimensions. The neighbor search list was updated every 10 steps. A constant temperature of 300 K was maintained using the Berendsen algorithm [42] and a coupling time of 0.1 ps, coupling independently the water and the protein to an external bath. A pressure of 1 bar was maintained isotropically, using the Berendsen pressure coupling scheme [42] with a time constant of 4 ps. Bond lengths were constrained using the LINCS method [43]. A cutoff of 1.0 nm was applied for VdW interactions. Long-range electrostatic interactions were calculated according to the particle mesh Ewald (PME) method [44], using a cutoff of 1 nm. The reciprocal space interactions were evaluated on a 0.14 nm grid using B-splines of fourth order.

The model of the membrane domain was embedded into a pre-equilibrated POPC bilayer consisting of 512 lipid molecules using the inflategro method [45]. Berger lipids [46], converted into the format of the OPLS all-atom force field [47], following the procedure proposed by Neale [48], were used to describe the POPC molecules. The semi-isotropic Berendsen coupling scheme was used for pressure coupling, while other parameters were the same as applied in simulation of the N-terminus. Simulations were carried out for 35 ns.

## Results

### Pleckstrin homology domain

The theoretical possibility for the existence of a split pleckstrin homology (PH) domain on the N-terminus of TRPA1 that would be able to bind PIP2 was testet, as the function of TPR channels is regulated by PIP2 [49, 50], but not much is known about the interaction sites [19, 51]. Initially, existence of a split pleckstrin homology domain involved in PIP2 binding was hypothesized for TRPC3 channel [52]. However, the hypothesis that a split PH domain of TRPC3 and the split PH domain in PLC $\gamma$1 could together form a full PH domain could not be confirmed [53] as only the two isolated halves of the split PH domain of PLC $\gamma$1 lead to formation of a full PH domain.

To test if the predicted PH domain [51] could exist in TRPA1, we applied the search algorithm described for TRPC3 by van Rossum et al. to identify a potential hidden PH domain [52]. Sequence hybrids of N-terminal TRPA1 sequence and C-terminal domain of PLC $\gamma$1 PH domain were submitted to the conserved domain database [54] to query for the identification of a complete PH domain. We scanned the N-terminus of TRPA1 (M1 to D63 and S569 to Y714), with the exception of the region containing classical ankyrin repeats. We could identify one region, for which the union with the PLC $\gamma$1 split PH domain resulted in a putative complete PH domain (K591-M634). Four potential locations of hidden PH domain in TRPA1 sequence were predicted by Karashima et al. based on canonical PIP2-binding site of PH domains [K-Xn-(K/R)-X-R] [51]. However, multiple sequence alignment of mammalian sequences showed conservation at only two potential sites on TRPA1 (K442-K447 and K591-R604). The canonical fold of the PH domain consists of seven-stranded antiparallel β-sheets followed by an C-terminal α-helix [55]. Secondary structure prediction indicated only two regions on TRPA1 N-terminus with a β-strand propensity: K7 to S43 and A572 to T624.

This analysis indicated that the region of the 16th ankyrin repeat could potentially contain a hidden split PH domain. We created a model of the TRPA1 N-terminus in which the 16th ankyrin repeat was modeled as a PH domain to test this hypothesis. Analysis of the 20 ns simulation showed a very high RMSD for the putative split PH domain region. We observed a loss of beta-strand secondary structure leading to instability of three dimensional shape of the motif. These results and the fact that the split PH domain would replace one ankyrin within the ankyrin repeat domain suggested that the existence of a split PH domain on the N-terminus of TRPA1 is very unlikely.

### Ankyrin repeat

We constructed a 3D model of the N-terminus of TRPA1, in which the loop between 12th and 13th ankyrin repeat is represented by the EF-hand domain which showed that these structural elements can coexist without affecting the canonical ankyrin repeat structure. The N-terminal domain of TRPA1 is unique among TRP channels: it contains a large number of ankyrin repeats, a common protein motif implicated, e.g., in protein-protein interactions, cell-cell signaling, elasticity, and molecular springs.

Ankyrin repeats are highly conserved. In the present work we built a homology model of the TRPA1 N-terminus containing 17 ankyrin repeats, using the structure of human ankyrinR [23] (PDB ID: 1N11) as a template. The structure of the ankyrinR template, which contains 12 repeats, was doubled at the site of the EF-hand and then truncated to 17 repeats. Figure 1a shows the structure of the N-terminal 17 ankyrin repeats. The model formed a canonical horseshoe structure containing 33 residues per ankyrin repeat. The best model showed good quality stereochemistry with 82.4% of the residues in the most favored region of the Ramachandran plot, while the overall g-factor showed a value of -0.19.

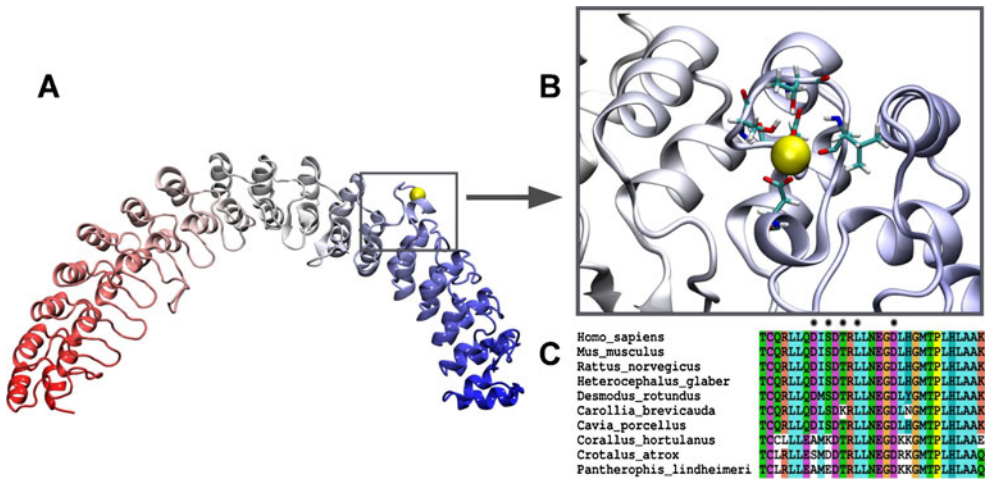


**Fig. 1** Panel **a** shows the structure of the 17 ankyrin repeat, color code red to blue from N- to C-terminus. The calcium ion is shown in yellow. Panel **b** shows the calcium ion bound to the EF-hand between ankyrin repeat 12 and 13. The side chains of those residues are shown, which coordinate the calcium ion. Panel **c** shows an alignment of TRPA1 sequences. Residues coordinating the calcium ion are conserved

Intracellular calcium has been reported to play an important role in the regulation of TRPA1. An important step toward understanding calcium-dependent regulation has been the identification of an EF-hand at the N-terminus [6]. The EF-hand is a widely distributed motif for calcium-binding. However, sequence analysis did not predict the existence of a classical EF-hand in TRPA1, but rather a calcium-binding loop, located between the 12th and the 13th ankyrin repeat. Nevertheless, experimental results have indicated the importance of the motif for channel regulation by intracellular calcium [17, 18]. Residues D468 and D479 have been described to be required for calcium-binding. This is in line with classical EF-hand properties, where the last residue of the EF-hand motif (D479 in TRPA1) is the most conserved and provides two oxygens for calcium binding. In addition, some decrease in response to calcium has been observed for S470 and Y472 [18]. In contrast, Doerner et al. reported only L474 to be critical for the sensitivity of TRPA1 to the calcium [17]. We have now identified an EF-hand calcium-binding motif in TRPA1 between ankyrin repeat 12 and 13. It is located between residues D468 and D479 and consists of 12 residues arranged in a helix-loop-helix structure. The above described residues (D468, S470, Y472, L474 and D477) correspond to five positions (1, 3, 5, 7 and 12) characteristic of classical EF-hands (Fig. 1b).

Sequence similarity, conservation and amino acid types in helices of the ankyrin repeats next to the calcium-binding site (as shown in Fig. 1c) pointed us to speculate that the canonical ankyrin repeat structural assembly might be maintained in the calcium-free structure. The calcium-free state is the ground state, as intracellular calcium concentration in resting cells is very low. The helices of the EF-hand are almost parallel. Although atypical of EF-hands, a similar helix – helix arrangement has been observed, for example, in grancalcin [56]. The template (PDB ID: 1XK4) for modeling the EF-hand was selected by comparing EF-hand sequences from different protein families available in the EF-hand Calcium-binding Proteins Data Library [http://structbio.vanderbilt.edu/cabp_database/]. The EF-hand region was initially aligned with the template using ClustalW and the resulting alignment was manually edited. The alignment of the EF-hand region was then fused with the alignment of the complete ankyrin repeat domain.

## Consequences of calcium-binding

We set out to ascertain whether calcium-binding affects the local geometry and helical arrangement, and whether the interactions in the core of the ankyrin repeat structure are strong enough to counteract conformational constraints resulting from calcium binding. 'Conformational selection' postulates that all protein conformations pre-exist, and the ligand selects the most favored conformation for binding [57]. As a consequence the ensemble undergoes a population shift, redistributing the conformational states. We docked calcium into the EF-hand, and used molecular dynamics simulations to probe for structural and dynamical effects of calcium-binding in our case. Simulations were carried out with and without calcium. The simulations were stable and showed well conserved secondary structure elements (see supplementary Fig. 4 of online material 1). Panel C to E of Fig. 2 show the observed global shapes of the N-terminus of TRPA1 and the end-to-end distance plot, measured from K108 (ankyrin repeat 2) to K593 (ankyrin repeat 16) quantifying the change in distances as a measure of the transition of the global conformations. The global horse shoe shape of the ankyrin repeat structure was maintained

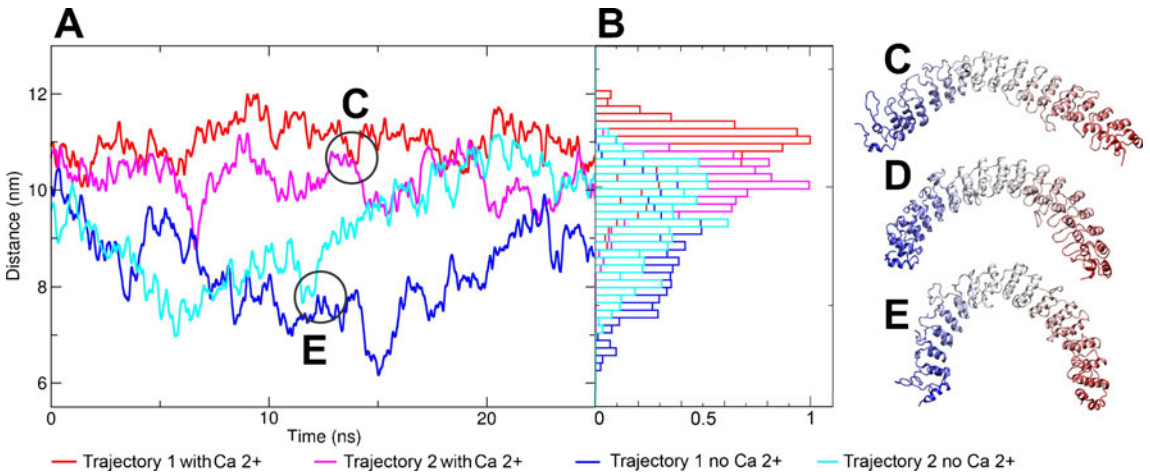


**Fig. 2** Analysis of the distance between K108 (ankyrin repeat 2) and K593 (ankyrin repeat 16). Panel **a** shows the time evolution of our simulations. Panel **b** shows a histogram of observed distances of panel **a**, using the same color coding. Panel **c**, **d** and **e** show representative structures: **c** extend structure of the calcium-bound state, **d** starting structure of our simulation, and **e** structure from the calcium-free simulations with short end-to-end distance. The circles indicate the position within the trajectories, from which the structures were taken

in the calcium free simulations, but we observed large fluctuations and, on average, a shrinkage in the end-to-end distance as compared to the starting model. When calcium is bound in the implanted EF-hand the ankyrin repeat structure stays stable in an extended horse shoe conformation. The larger fluctuations in calcium-free simulations which also sampled calcium-bound conformations suggested a more dynamic behavior of the ankyrin repeat domain. Calcium "selects" the extended horse shoe conformation from the ensemble of conformational states and the ensemble undergoes a population shift with the end-to-end distance in the calcium-bound structures on average larger by ~1.85 nm.

In order to better compare the dynamic changes of all simulations we carried out principal component analysis (see Fig. 3). Simulations were fitted to a common references frame, fitting to the helices of the first 11 ankyrin repeats, because the global shape of those helices remains very similar in all simulations. Motions of each simulation were projected onto the same two largest eigenvectors in order to allow for direct comparison [58]. We found a clear separation between the calcium-bound and the calcium-free simulations, showing that indeed an only partially overlapping phase space was sampled. Both calcium-bound simulations converged to the same area suggesting sufficient sampling. Similar observations were made for the calcium-free simulations. The sampled phase space of both calcium-free simulations showed that a larger area was sampled, consistent with the observation from the end-to-end distance plot (see Fig. 2). Both sets of simulations showed strong sampling along the first eigenvector, which describes the extension of the structure along of the end-to-end distance vector; with a clear separation: calcium-free simulation partitioned toward lower values, while simulations of calcium-bound ankyrin repeats showed a transition toward higher values. The projection of the calcium-free simulations indicated that the

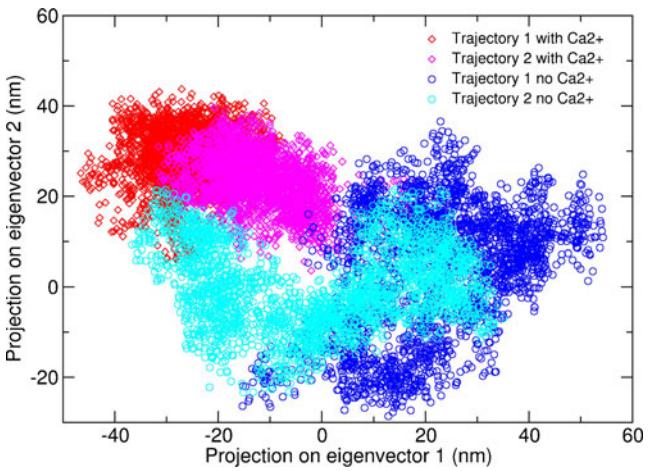


**Fig. 3** Projection of the simulations into a common framework of the first two largest eigenvectors. Eigenvector 1 describes the extension of the ankyrin repeat, eigenvector two a change in the superhelicity

motion along eigenvector one has an amplitude that is twice as large as in the calcium-bound state. The shape of the ankyrin repeats is therefore much less constrained and can reach a stretched conformation that is similar to the calcium-bound state.

Eigenvector two describes a change in the super-helicity normal to the end-to-end connecting line. We observed that the calcium-bound simulations display a much smaller range of sampling along eigenvector two as compared to the calcium-free state. We again observed that the calcium-free simulations show overlap with the calcium-bound, but largely sample additional phase space.

Largest changes in bending are present in the area around the EF-hand for both eigenvectors, indicating that the local changes induced by calcium-binding do directly translate in a selection of an overall shape. Calcium-binding has, indeed, been shown to increase ion flux through the TRPA1 channel. We observe that insertion of calcium to the EF-hand between ankyrin repeats 12 and 13 induces a change in the helix-helix crossing angle. Figure 4a shows the parallel arrangement of ankyrin repeat helices in the calcium free state to the EF-hand. The local geometry changes are promoted by coordination of the calcium ion. Residue D479 on ankyrin repeat 13 is maintained in closer proximity to D405 on the second helix of ankyrin repeat 12 in the calcium bound state, thereby promoting the rotation of ankyrin repeat 13 relative to the preceding ankyrin repeat. Figure 4b shows the change in distance between ankyrin repeat 12 and 13. We observe that this distance is 0.52 nm longer in the calcium free simulations than if constrained by calcium binding to the EF-hand. This small local change becomes amplified by the extended ankyrin repeat structure and translated into the large population shift in end-to-end distance.

## Binding of chemical irritants

The TRPA1 channel is known to sense irritant chemical substances that are hydrophobic in nature and readily react with sulfhydryl groups [6, 16, 59–61]. The human TRPA1 possess 20 cysteine residues in its N-terminus. Three of them have been found to react with isothiocyanates [6]. Two of these cysteines, C621 and C641, are located close in space on the 17th ankyrin repeat (see Fig. 5), while the third cysteine residue (C665) is in close proximity in sequence. Experimental data indicate that all three cysteines contribute similarly to the effect of chemical irritants. We did not predict the structure of the TRPA1 N-terminus following the 17th ankyrin repeat, because we focused on the ankyrin repeats. Ankyrin repeats at the edges of the ankyrin repeat domain are often less conserved then those in the middle [3], but the sequence after the 17th repeat did not show any sequence similarity to an ankyrin repeat. The

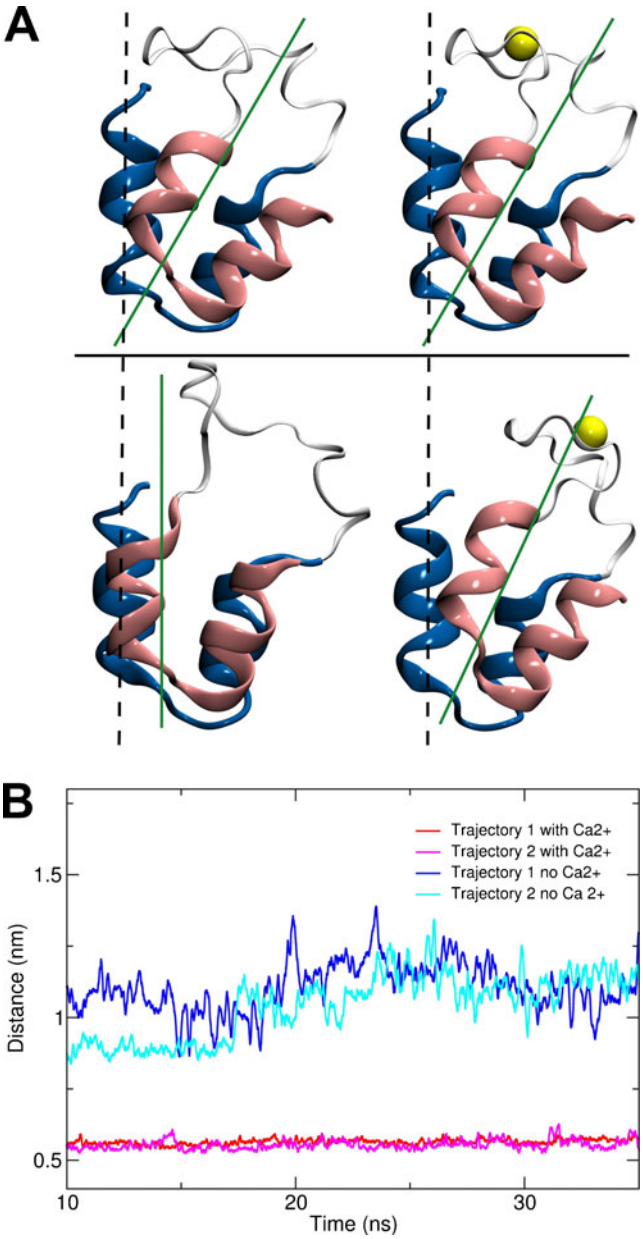


**Fig. 4** Panel **a** shows the relative orientation of ankyrin repeat 12 and 13. The upper structures are the start structures of the simulations, the lower structures are taken from the last frame. The left side shows the structures from the apo simulation and the structures for the right figures are taken from the simulation with bound calcium. Panel **b** shows the change in the distance between D405 and D416, reflecting the difference in orientation of ankyrin repeat 12 vs. ankyrin repeat 13

16th and 17th ankyrin repeats differ already from the classical pattern, supporting our interpretation of domain termination after repeat number 17. Although we did not build a structure following the 17th ankyrin repeat the exposed hydrophobic surface of the last ankyrin repeat suggested that the polypeptide chain should fold against it. We can therefore, in light of the experimental data, assume that C665 should be located next to C621 and C641.

## Transmembrane domain

TRPA1 is a non-selective cation channel with topology predicted to be similar to potassium channels consisting of six transmembrane helices (S1-S6) and a pore formed between the fifth and the sixth helix. We created a model of the TRPA1 transmembrane domain using the crystal structure of Kv1.2 potassium channel [32] (PDB ID: 3LUT) as a template. The best model, selected by applying the Yasara Z-score and Ramachandran plot analysis, was inserted into a pre-equilibrated membrane as described in material and methods. After system equilibration, a simulation of 30 ns was carried out. The global structure of the TRPA1 channel remained stable over this time window, showing a RMSD for the Cα atoms of 0.6 nm, and a stable secondary structure (supplementary Fig. 5 of online material 1), indicating correctness of the model.

Calcium ions play a key role in channel regulation, as they can inactivate the channel by blocking the ion permeation path at negative membrane potential of -80 mV [62], while more positive potential above -20 mV can unblock the channel. The residue D915 aligned with the analogue aspartate D379 of Kv1.2. We found this residue to be part of the selectivity filter. Mutation of D915 has been shown to reduce the calcium permeability through the channel [63]. The same residue, if mutated, abolishes zinc permeation [64]. Our model shows that D915 is located at the entrance of the pore. It forms a ring of negative charges that are exposed to the extracellular solvent and can therefore attract cations.

Figure 6b shows a zoom onto the amphiphilic helix connecting S4 with S5. Residue N855, which is in the loop between S4 and the S4-S5 connecting helix, is associated with familial episodic pain syndrome [65]. In this hereditary disease, N855 is mutated to serine. Residue N855 seems to have a role in strengthening the interaction between S1 and

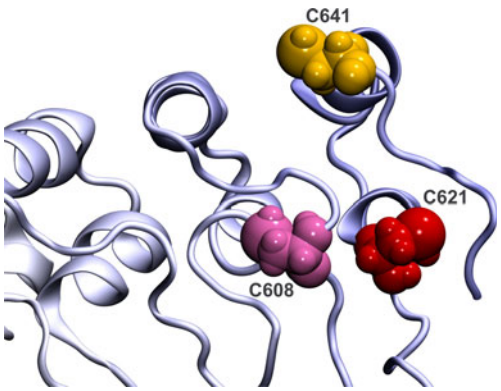


**Fig. 5** Residues C608 (pink), C621 (red) and C641 (orange), all chemically modified by irritants, are located on ankyrin repeat 16 and 17 and can be found in close proximity. Residues C608 and C621, which have been found to form disulfide bounds [72] are in close contact

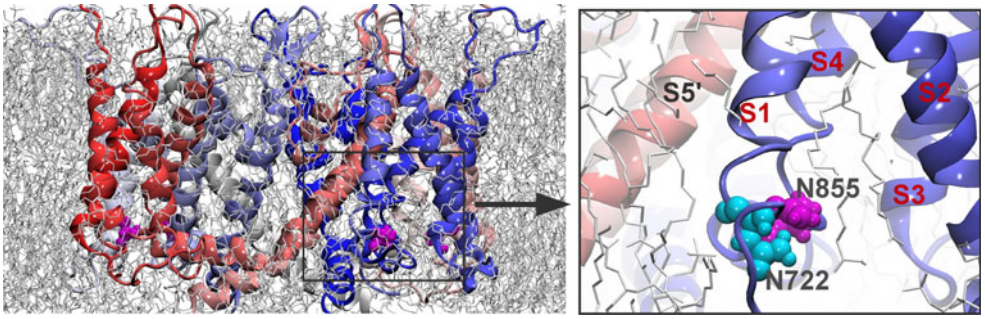


**Fig. 6** Transmembrane domain of TRPA1. Panel **a** shows the membrane inserted channel. The four subunits are colored differently. Residue N855 is highlighted in magenta. Panel **b** shows a zoom onto N855, which is at the turn between S4 and the S4-S5 linker helix. The side chain of N855 forms stable interactions with S1

the S4-S5 connecting helix. We observed, in all four TRPA1 subunits, stable hydrogen bonds between the side chain of N855 and the N-terminus of S1, especially with N724 located on the N-terminus of S1, while the other interactions with the S1 helix are hydrophobic in nature. This interaction does create a direct link between the N-terminus and the S4-S5 connecting helix. The serine side chain of the mutant is less polar and has a lower hydrogen bonding capability, therefore weakening the hydrogen bonds between the two helices, and as a consequence, loosening the mechanical coupling to the ankyrin repeats.

Structural assembly

A 16 Å resolution structure of TRPA1, resolved by single-particle cryo-electron microscopy (cryo-EM) has recently been reported [66]. The cryo-EM map shows the tetrameric architecture of the channel. The transmembrane and the intracellular domains are clearly visible. Together with the EM structure of TRPA1 a homology model of the channel was proposed by Cvetkov et al. [64], consisting of a 12 ankyrin repeat N-terminus, the transmembrane domain and the C-terminus. Although our model lacks the C-terminal domain, as the low sequence similarity does not allow to generate a model suitable for molecular dynamics simulations and therefore cannot be compared here, the N-terminus model in our case stays on a 17 ankyrin repeat structure based on theoretical predictions. Both transmembrane models are based on the potassium Kv1.2 structure containing six transmembrane domains with a pore loop between the fifth and sixth TM domain. We separately fitted our models of the TRPA1 N-terminus and the TM domain into the cryo-EM map using Chimera/Segger [67, 68], applying the same volume threshold, that corresponds to a protein molecular mass of 525 kDa, as used by Cvetkov et al. [66]. The TM domain was fitted in its tetrameric assembly into the density map. We observe a similar fit of the transmembrane domain into the density map as previously reported. The N-terminal 17 ankyrin repeat domain was first fitted as a single monomeric molecule, followed by reconstruction of the full tetrameric assembly by symmetry operations using the Chimera tools. A representative snapshot based on end-to-end distance from both the calcium-bound as well as from the calcium-free ankyrin repeats simulation was selected. We were able to place both structures into the hanging basket architecture of the TRPA1 cryo-EM density map, but obtained a better fit with the model of the calcium-bound ankyrin repeat. The fitted conformations of the 17 ankyrin repeat structures, as shown in Fig. 7, differ between the calcium-bound and the calcium-free state, as curvature and end-to-end distance are not the same. However, both models fit satisfactorily into the curve shape of the density map, while leaving additional space at the bottom, thereby allowing to accommodate the first 62 N-terminal residues not included in our model.

## Discussion

TRPA1 is the only mammalian channel that carries more than 10 ankyrin repeats on its N-terminus. It is expressed only in the inner ear and in the nociceptive nerve system. TRPA1 is important in sensing of pain, and has been associated with several functions, including hearing, sensing of mechanical stress, and detection of chemical irritants. Several interaction sites, most of them on the long intracellular N-terminus, have been identified. Figure 8 shows a schematic view of TRPA1. Ankyrin repeats are known protein-protein interacting domains, which can also serve as molecular springs, due to their elastic nature. The spring constant and the stretchability of the ankyrin repeat have been determined, showing that the ankyrin repeat structure can extend by 6-7 nm while maintaining structural integrity [4, 9]. In order to control the function of the TRPA1 channel, the force on the ankyrin repeats must be propagated to the pore and gate. The force, as shown in Fig. 7, can directly propagate from the ankyrin repeat to the inner gate via the S1-S4 domain and the amphiphilic S4-S5 connecting helix. The following sites on TRPA1, which can modulate the open probability of the channel are shown: i) the calcium-binding EF-hand, ii) the binding site for irritants, which activate the channel by covalent modification of cysteine residues and iii) the site of the N855S mutation that is associated with familial episodic pain syndrome [65].

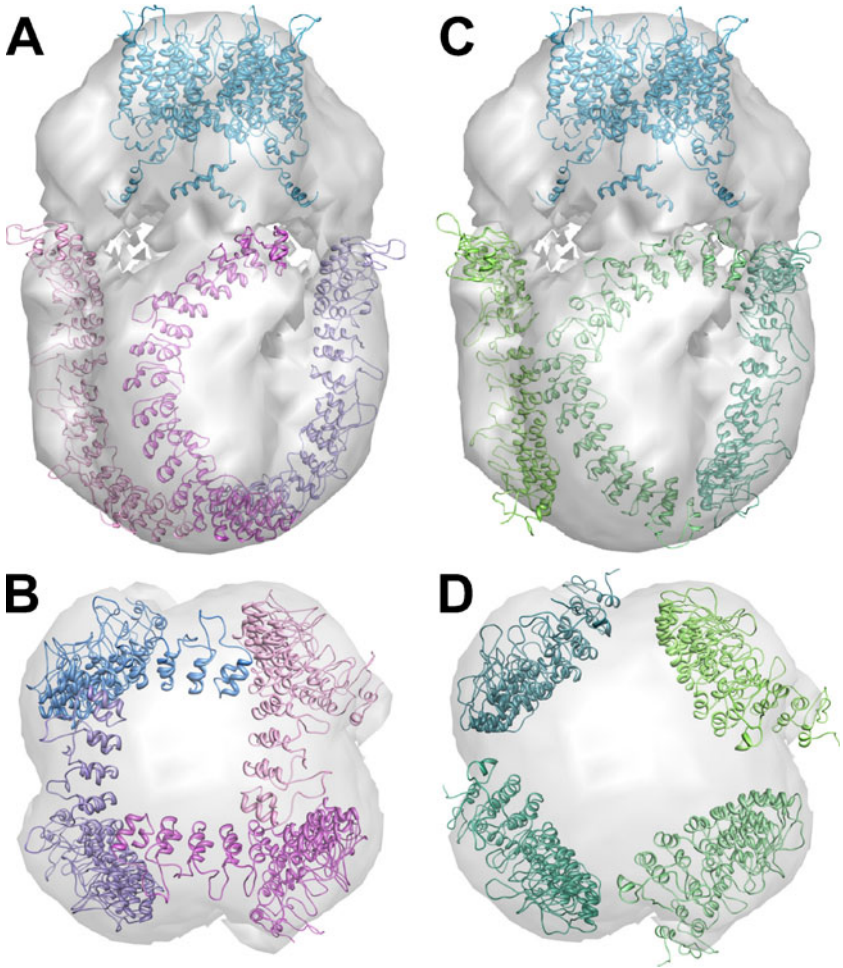


**Fig. 7** A fit of our models representing the transmembrane and the N-terminal domain of TRPA1 into the recently published Cryo-EM map [66] is shown from the membrane and the intracellular site. Panels **a** and **b** show the fit of the calcium-free N-terminus, panels **c** and **d** show the calcium-bound state from a side and an intracellular view, respectively. The density map is shown in gray using the volume threshold, which corresponds to the molecular mass of TRPA1

The apo state is characterized by large fluctuations of the end-to-end distances, as we observe a fluctuation amplitude of almost 50% of its total length. We find that binding of calcium to the EF-hand stiffens the ankyrin repeat structure and selects for the long overall end-to-end distance. Similar observations of a selection of a conformation by ligand binding from a strongly fluctuating apo state have been made in the arginine repressor [69]. It is predicted that a net effect of this change in the ankyrin repeat property is a change of the force acting on the gate. Calcium-binding to the EF-hand has been shown to open the channel at low membrane potential. Only at a negative membrane potential of -80 mV can inactivation be observed, thought to occur by direct blockage of the ion permeation pore [60, 70, 71].

It is unknown what the structural effects are of reversible covalent binding to cysteines by hydrophobic pungent molecules like the active compounds diallyl disulfide in garlic, allyl isothiocyanate of mustard oil and cinnamaldehyde [6, 59–61]. It is tempting to speculate that chemical modification of C621, C641 and C665 could lead to an alteration of the local structure and hydrophobic interactions in the small domain (approximately from residue 645 to 715) between

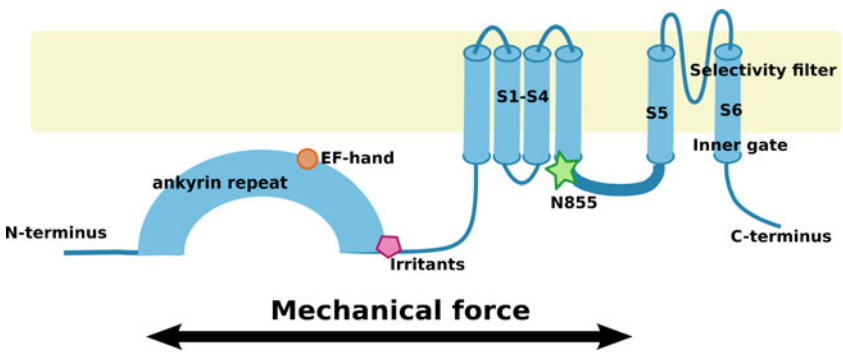


**Fig. 8** Model of TRPA1 activation. The ankyrin repeats and those sites are marked that are known to affect the open probability of the channel

the ankyrin repeats and the S1-S4 domain. The effect of cysteine modification has been shown to be cumulative [6], indicating an increasing probability of structural changes with increasing chemical modification. It is likely that the compactness of this region changes, which under mechanical force translates into a modification of the forces acting from the N-terminus on the gate.

The familial episodic pain syndrome associated with mutation N855S does not alter the maximum ion flux through TRPA1, but increases the open probability of the channel. We observe in our simulation of the TM domain of the TRPA1 (S1 to S6) channel that N855 does form a strong interaction with the N-terminus of S1. This interaction, visible in all four subunits, effectively creates a direct force-link between the N-terminus and the S4-S5 linker helix, and therefore to the gate. The N855S mutation weakens this interaction. The net effect is therefore a reduction of the mechanical force by which the N-terminus pulls on the gate.

Very different signals can activate TRPA1 in the nociceptive nerve system. It would be difficult to envision an ion channel in which every different signal could activate the channel by a completely independent mechanism. We propose the existence of a single force transduction path, which is activated by possibly all signals that act via the N-terminus of TRPA1. The dimension of the N-terminal structure (from the ankyrin repeat via the S1-S4 domain to the gate) allows to integrate several switches. These switches represent interaction sites for the different physiological signals recognized by TRPA1, such as force, ions or chemical irritants. All these sites translate the binding event into a mechanical signal that acts on the gate. Opening of the gate then allows ion flux and generation of a nerve impulse [49].

The N-terminus of TRPA1 is not the sole interaction site for signal creation. TRPA is regulated by the signaling lipid PIP2, but the interaction site is unknown. We tested the possibility of the existence of a split PH domain within the N-terminus. Our efforts suggest that the putative split PH domain most likely does not exist. The interaction with PIP2 therefore probably involves a mechanism other than formation of an intermolecular split PH domain.

The voltage sensing region has been identified within the C-terminus of TRPA1, and has been found to be sensitive to allyl isothiocyanate at relatively high doses [70, 71]. Recently, direct activation of TRPA1 channel by intracellular zinc has been reported [64]. It has been demonstrated that the C641 residue within the N-terminus, as well as the H983 and C1021 residues within the C-terminus are involved in Zn-dependent TRPA1 activation. Mutations of C641 modestly reduce the dependency of the channel function on zinc, while mutations of the two residues identified at the C-terminus show a strong effect. Our structural analysis of the N-terminal domain predict that the residues C621, C641 and H644 are located very close in space (see Fig. 5). It is conceivable that C665 is also located in close proximity. These residues might represent a weak zinc binding site.

Recently, disulfide bridges between the cysteine C665 and C621, C665 and C462, C665 and C192, as well as C621 and C608 have been observed using mass spectroscopy [72]. Our 17 ankyrin repeat model (see Fig. 5) of the N-terminus shows that residues C621 and C608 are indeed next to each other, showing an average Cα distance of 0.69 nm. Cysteine 665 is 17 residues from the C-terminus of our ankyrin repeat model, which terminates with residue D648. We can therefore only speculate about the position of C665. The experimentally observed disulfide bond between C665 and C192 is difficult to reconcile with our TRPA1 model, because we find that the two residues are on opposing ends in structures fitted into the EM density map of the intracellular N-terminal domain. A close association between C665 and C621 seems possible, given the proximity in sequence. Residue C462 is on the same ankyrin repeat structure most likely to be distant from D648, therefore precluding a close association with C665 even if the sequence stretch between D648 and C665 is completely extended. On the other site, C462 on the next protomer is just apposed to the ankyrin repeat number 17, suggesting that C462 and C665 could be in contact. We observe distances of 6.1 nm (calcium free) and 6.9 nm (calcium bound) between the Cα atoms of C621 and C462 on the adjacent N-terminus, measured in our models that were fitted into the electron density map. This indicates that two conformations should exist, which differ in the distance between C665 and C621, and between C665 and C462, because even if we take the large uncertainty of fitting our model into the 16 Å Cryo-EM density map into account, it is difficult to envision that C665 could be simultaneously close to both residues.

The TRPA1 channel has been associated with creation of an electrical signal from the vibrations of the stereocilia in the inner ear [73–75]. Tension on the TRPA1 channel is created and maintained by myosin-1c, which holds the channel at its most sensitive point [76–78]. Ankyrin repeats have been predicted to possess biophysical properties that would match the experimentally measured properties of the gating spring in the inner ear [4, 79]. We predict that the TRPA1 channel in nociceptive neurons uses a similar principle for function as involved in hearing. The channel is gated by several different stimuli acting on its N-terminus. While in hearing, the vibrations of the stereocilia are translated into an electrical signal, in nociceptive neurons the different stimuli modify the length of the N-terminus, thereby changing the force acting on the gate and as a consequence changing the open probability of the TRPA1 channel.

## Conclusions

We have developed a unifying model of TRPA1 gating by mechanical force, chemical modification by irritants, calcium-binding, and zinc-binding. The N-terminus senses physiological signals, and acts as a mechanical spring that connects directly to the gate. The ankyrin repeats play a central role in controlling the open probability of the gate by acting as soft springs. The ankyrin repeats can be extended by several nm without unfolding. Even if overstretched, they have been shown to spontaneously refold [4, 9]. These properties allow the ankyrin repeat domain to fine-tune the force acting on the channel, and at the same time to act as a security net against mechanical damage. Our model predicts that the different physiological signals acting via the N-terminus all affect TRPA1 function by transducing mechanical force to the gate.

**Acknowledgments** We gratefully acknowledge support from the Ministry of Education, Youth and Sports of the Czech Republic (projects No. ME09062 and MSM6007665808), the Academy of Sciences of the Czech Republic (AVOZ60870520), and the Czech Science Foundation, grant P207/10/1934. VZ is supported by the University of South Bohemia, grant GAJU 170/2010/P. Access to the National Grid Infrastructure -MetaCentrum- is highly appreciated.

## References

1. Story GM, Peier AM, Reeve AJ, Eid SR, Mosbacher J, Hricik TR, Earley TJ, Hergarden AC, Andersson DA, Hwang SW et al. (2003) ANKTM1, a TRP-like channel expressed in nociceptive neurons, is activated by cold temperatures. Cell 112:819–829
2. Corey DP, García-Añoveros J, Holt JR, Kwan KY, Lin SY, Vollrath MA, Amalfitano A, Cheung ELM, Derfler BH, Duggan A et al. (2004) TRPA1 is a candidate for the mechanosensitive transduction channel of vertebrate hair cells. Nature 432:723–730
3. Gaudet R (2008) A primer on ankyrin repeat function in TRP channels and beyond. Mol Biosyst 4:372–379
4. Sotomayor M, Corey DP, Schulten K (2005) In search of the hair-cell gating spring elastic properties of ankyrin and cadherin repeats. Structure 13:669–682
5. García-Añoveros J, Nagata K (2007) TRPA1. Handbook of experimental pharmacology. doi:10.1007/978-3-540-34891-7_21
6. Hinman A, Chuang HH, Bautista DM, Julius D (2006) TRP channel activation by reversible covalent modification. Proc Natl Acad Sci USA 103:19564–19568
7. Lux SE, John KM, Bennett V (1990) Analysis of cDNA for human erythrocyte ankyrin indicates a repeated structure with homology to tissue-differentiation and cell-cycle control proteins. Nature 344:36–42
8. Breeden L, Nasmyth K (1987) Similarity between cell-cycle genes of budding yeast and fission yeast and the Notch gene of Drosophila. Nature 329:651–654
9. Lee G, Abdi K, Jiang Y, Michaely P, Bennett V, Marszalek PE (2006) Nanospring behaviour of ankyrin repeats. Nature 440:246–249
10. Cavanaugh EJ, Simkin D, Kim D (2008) Activation of transient receptor potential A1 channels by mustard oil, tetrahydrocannabinol and Ca2+ reveals different functional channel states. Neuroscience 154:1467–1476
11. Macpherson LJ, Dubin AE, Evans MJ, Marr F, Schultz PG, Cravatt BF, Patapoutian A (2007) Noxious compounds activate TRPA1 ion channels through covalent modification of cysteines. Nature 445:541–545
12. Sawada Y, Hosokawa H, Matsumura K, Kobayashi S (2008) Activation of transient receptor potential ankyrin 1 by hydrogen peroxide. Eur J Neurosci 27:1131–1142
13. Taylor-Clark TE, Kiros F, Carr MJ, McAlexander MA (2009) Transient receptor potential ankyrin 1 mediates toluene diisocyanate-evoked respiratory irritation. Am J Resp Cell Mol 40:756–762
14. Birrell MA, Belvisi MG, Grace M, Sadofsky L, Faruqi S, Hele DJ, Maher SA, Freund-Michel V, Morice AH (2009) TRPA1 agonists evoke coughing in guinea pig and human volunteers. Am J Respir Crit Care 180:1042–1047
15. Taylor-Clark TE, Undem BJ (2010) Ozone activates airway nerves via the selective stimulation of TRPA1 ion channels. J Physiol 588:423–433
16. Bessac BF, Sivula M, von Hehn CA, Caceres AI, Escalera J, Jordt SE (2009) Transient receptor potential ankyrin 1 antagonists block the noxious effects of toxic industrial isocyanates and tear gases. FASEB J 23:1102–1114
17. Doerner JF, Gisselmann G, Hatt H, Wetzel CH (2007) Transient receptor potential channel A1 is directly gated by calcium ions. J Biol Chem 282:13180–9
18. Zurborg S, Yurgionas B, Jira JA, Caspani O, Heppenstall PA (2007) Direct activation of the ion channel TRPA1 by Ca2+. Nat Neurosci 10:277–279
19. Kim D, Cavanaugh EJ, Simkin D (2008) Inhibition of transient receptor potential A1 channel by phosphatidylinositol-4,5-bisphosphate. Am J Physiol Cell Ph 295:C92–99
20. Dai Y, Wang S, Tominaga M, Yamamoto S, Fukuoka T, Higashi T, Kobayashi K, Obata K, Yamanaka H, Noguchi K (2007) Sensitization of TRPA1 by PAR2 contributes to the sensation of inflammatory pain. J Clin Invest 117:1979–1987
21. Li L, Wetzel S, Plückthun A, Fernandez JM (2006) Stepwise unfolding of ankyrin repeats in a single protein revealed by atomic force microscopy. Biophys J 90:L30–2
22. Serquera D, Lee W, Settanni G, Marszalek PE, Paci E, Itzhaki LS (2010) Mechanical unfolding of an ankyrin repeat protein. Biophys J 98:1294–1301
23. Michaely P, Tomchick DR, Machius M, Anderson RGW (2002) Crystal structure of a 12 ANK repeat stack from human ankyrinR. EMBO J 21:6387–6396
24. Rost B, Yachdav G, Liu J (2004) The predictprotein server. Nucleic Acids Res 32:W321–6
25. Söding J, Biegert A, Lupas AN (2005) The HHpred interactive server for protein homology detection and structure prediction. Nucleic Acids Res 33:W244–248
26. Zhang Y (2008) I-TASSER server for protein 3D structure prediction. BMC Bioinforma 9:40
27. Bennett-Lovsey RM, Herbert AD, Sternberg MJE, Kelley LA (2008) Exploring the extremes of sequence/structure space with ensemble fold recognition in the program Phyre. Proteins 70:611–625
28. Larkin MA, Blackshields G, Brown NP, Chenna R, McGettigan PA, McWilliam H, Valentin F, Wallace IM, Wilm A, Lopez R et al. (2007) ClustalW and ClustalX version 2. Bioinformatics 23:2947–2948
29. Sali A, Blundell TL (1993) Comparative protein modeling by satisfaction of spatial restraints. J Mol Biol 234:779–815
30. Korndörfer IP, Brueckner F, Skerra A (2007) The crystal structure of the human (S100A8/S100A9)2 heterotetramer, calprotectin, illustrates how conformational changes of interacting alpha-helices can determine specific association of two EF-hand proteins. J Mol Biol 370:887–898

31. Laskowski RA, MacArthur MW, Moss DS, Thornton JM (1993) PROCHECK: a program to check the stereochemical quality of protein structures. J Appl Crystallogr 26:283–291
32. Wiederstein M, Sippl MJ (2007) ProSA-web: interactive web service for the recognition of errors in three-dimensional structures of proteins. Nucleic Acids Res 35:W407–10
33. Chen X, Wang Q, Ni F, Ma J (2010) Structure of the full-length Shaker potassium channel Kv1.2 by normal-mode-based X-ray crystallographic refinement. Proc Natl Acad Sci USA 107:11352–11357
34. Sonnhammer EL, von Heijne G, Krogh A (1998) A hidden Markov model for predicting transmembrane helices in protein sequences. Proc Int Conf Intell Syst Mol Biol 6:175–182
35. Hofmann K, Stoffel W (1993) TMBASE - a database of membrane spanning protein segments. Biol Chem 374:166–170
36. Notredame C, Higgins DG, Heringa J (2000) T-Coffee: a novel method for fast and accurate multiple sequence alignment. J Mol Biol 302:205–217
37. Edgar RC (2004) MUSCLE: a multiple sequence alignment method with reduced time and space complexity. BMC Bioinforma 5:113
38. Krieger E, Koraimann G, Vriend G (2002) Increasing the precision of comparative models with YASARA NOVA–a self-parameterizing force field. Proteins 47:393–402
39. Berendsen HJC, Postma JPM, van Gunsteren WF, Hermans J (1981) In: Intermolecular Force. B. Pullman (ed.), Reidel, Dordrecht, pp 331-342
40. Hess B, Kutzner C, van der Spoel D, Lindahl E (2008) GROMACS 4: algorithms for highly efficient, load-balanced, and scalable molecular simulation. J Chem Theor Comput 4:435–447
41. Van Der Spoel D, Lindahl E, Hess B, Groenhof G, Mark AE, Berendsen HJC (2005) GROMACS: fast, flexible, and free. J Comput Chem 26:1701–1718
42. Berendsen HJC, Postma JPM, van Gunsteren WF, DiNola A, Haak JR (1984) Molecular dynamics with coupling to an external bath. J Chem Phys 81:3684–3690
43. Hess B, Bekker H, Berendsen HJC, Fraaije JGEM (1997) LINCS: a linear constraint solver for molecular simulations. J Comput Chem 18:1463–1472
44. Darden T, York D, Pedersen L (1993) Particle mesh Ewald: an N·log(N) method for Ewald sums in large systems. J Chem Phys 98:10089–10092
45. Kandt C, Ash WL, Tieleman DP (2007) Setting up and running molecular dynamics simulations of membrane proteins. Methods 41:475–488
46. Berger O, Edholm O, Jahnig F (1997) Molecular dynamics simulations of a fluid bilayer of dipalmitoylphosphatidylcholine at full hydration, constant pressure, and constant temperature. Biophys J 72:2002–2013.47
47. Jorgensen WL, Maxwell DS, Tirado-Rives J (1996) Development and testing of the OPLS all-atom force field on conformational energetics and properties of organic liquids. J Am Chem Soc 118:11225–11236
48. http://lists.gromacs.org/pipermail/gmx-developers/2008-March/002422.html and http://www.pomeslab.com/files/lipidCombinationRules.pdf
49. Nilius B, Owsianik G, Voets T (2008) Transient receptor potential channels meet phosphoinositides. EMBO J 27:2809–2816
50. Qin F (2007) Regulation of TRP ion channels by phosphatidylinositol-4,5-bisphosphate. Handbook of experimental pharmacology. doi:10.1007/978-3-540-34891-7_30
51. Karashima Y, Prenen J, Meseguer V, Owsianik G, Voets T, Nilius B (2008) Modulation of the transient receptor potential channel TRPA1 by phosphatidylinositol 4,5-biphosphate manipulators. Pflügers Arch: E J Physiol 457:77–89
52. van Rossum DB, Patterson RL, Sharma S, Barrow RK, Kornberg M, Gill DL, Snyder SH (2005) Phospholipase Cgamma1 controls surface expression of TRPC3 through an intermolecular PH domain. Nature 434:99–104
53. Wen W, Yan J, Zhang M (2006) Structural characterization of the split pleckstrin homology domain in phospholipase C-gamma1 and its interaction with TRPC3. J Biol Chem 281:12060–8
54. Marchler-Bauer A, Panchenko AR, Shoemaker BA, Thiessen PA, Geer LY, Bryant SH (2002) CDD: a database of conserved domain alignments with links to domain three-dimensional structure. Nucleic Acids Res 30:281–283
55. Haslam RJ, Koide HB, Hemmings BA (1993) Pleckstrin domain homology. Nature 363:309–310
56. Jia J, Borregaard N, Lollike K, Cygler M (2001) Structure of Ca(2+)-loaded human grancalcin. Acta Crystallogr D 57:1843–1849
57. Boehr DD, Nussinov R, Wright PE (2009) The role of dynamic conformational ensembles in biomolecular recognition. Nat Chem Biol 5:789–796. doi:10.1038/nchembio.232
58. Stockner T, Vogel HJ, Tieleman DP (2005) A salt-bridge motif involved in ligand binding and large-scale domain motions of the maltose-binding protein. Biophys J 89:3362–3371
59. Jordt SE, Bautista DM, Chuang HH, McKemy DD, Zygmunt PM, Högestätt ED, Meng ID, Julius D (2004) Mustard oils and cannabinoids excite sensory nerve fibres through the TRP channel ANKTM1. Nature 427:260–265
60. Bandell M, Story GM, Hwang SW, Viswanath V, Eid SR, Petrus MJ, Earley TJ, Patapoutian A (2004) Noxious cold ion channel TRPA1 is activated by pungent compounds and bradykinin. Neuron 41:849–857
61. Bautista DM, Movahed P, Hinman A, Axelsson HE, Sterner O, Högestätt ED, Julius D, Jordt SE, Zygmunt PM (2005) Pungent products from garlic activate the sensory ion channel TRPA1. Proc Natl Acad Sci USA 102:12248–12252
62. Nagata K, Duggan A, Kumar G, García-Añoveros J (2005) Nociceptor and hair cell transducer properties of TRPA1, a channel for pain and hearing. J Neurosci 25:4052–4061
63. Wang YY, Chang RB, Waters HN, McKemy DD, Liman ER (2008) The nociceptor ion channel TRPA1 is potentiated and inactivated by permeating calcium ions. J Biol Chem 283:32691–32703
64. Hu H, Bandell M, Petrus MJ, Zhu MX, Patapoutian A (2009) Zinc activates damage-sensing TRPA1 ion channels. Nature Chem Biol 5:183–190
65. Kremeyer B, Lopera F, Cox JJ, Momin A, Rugiero F, Marsh S, Woods CG, Jones NG, Paterson KJ, Fricker FR et al. (2010) A gain-of-function mutation in TRPA1 causes familial episodic pain syndrome. Neuron 66:671–680
66. Cvetkov TL, Huynh KW, Cohen MR, Moiseenkova-Bell VY (2011) Molecular architecture and subunit organization of TRPA1 channel revealed by electron microscopy. J Biol Chem 286:38168–38176
67. Pettersen EF, Goddard TD, Huang CC, Couch GS, Greenblatt DM, Meng EC, Ferrin TE (2004) UCSF chimera - a visualization system for exploratory research and analysis. J Comput Chem 25:1605–1612
68. Pintilie GD, Zhang J, Goddard TD, Chiu W, Gossard DC (2010) Quantitative analysis of cryo-EM density map segmentation by watershed and scale-space filtering, and fitting of structures by alignment to regions. J Struct Biol 170(3):427–438
69. Strawn R, Melichercik M, Green M, Stockner T, Carey J, Ettrich R (2010) Symmetric allosteric mechanism of hexameric Escherichia coli arginine repressor exploits competition between L-arginine ligands and resident arginine residues. PLoS Comput Biol 6(6): e1000801
70. Benedikt J, Samad A, Ettrich R, Teisinger J, Vlachova V (2009) Essential role for the putative S6 inner pore region in the activation gating of the human TRPA1 channel. Biochim Biophys Acta 1793:1279–88.72

71. Samad A, Sura L, Benedikt J, Ettrich R, Minofar B, Teisinger J, Vlachova V (2010) The C-terminal basic residues contribute to the chemical- and voltage-dependent activation of TRPA1. Biochem J 433:197–204
72. Wang L, Cvetkov TL, Chance MR, Moiseenkova-Bell VY (2012) Identification of in vivo disulfide conformation of TRPA1 ion channel. J Biol Chem 287:6169–6176
73. Hudspeth AJ, Corey DP (1977) Sensitivity, polarity, and conductance change in the response of vertebrate hair cells to controlled mechanical stimuli. Proc Natl Acad Sci USA 74:2407–2411
74. Gillespie PG, Walker RG (2001) Molecular basis of mechanosensory transduction. Nature 413:194–202
75. Hudspeth AJ (1982) Extracellular current flow and the site of transduction by vertebrate hair cells. J Neurosci 2:1–10
76. Gillespie PG, Wagner MC, Hudspeth AJ (1993) Identification of a 120 kd hair-bundle myosin located near stereociliary tips. Neuron 11:581–94
77. García JA, Yee AG, Gillespie PG, Corey DP (1998) Localization of myosin-Ibeta near both ends of tip links in frog saccular hair cells. J Neurosci 18:8637–8647
78. Holt JR, Gillespie SKH, Provance DW, Shah K, Shokat KM, Corey DP, Mercer JA, Gillespie PG (2002) A chemical-genetic strategy implicates myosin-1c in adaptation by hair cells. Cell 108:371–381
79. Howard J, Hudspeth AJ (1988) Compliance of the hair bundle associated with gating of mechanoelectrical transduction channels in the bullfrog's saccular hair cell. Neuron 1:189–199